Wang, Yadong; Jiang, Biqiang; Das, Susobhan; Zhao, Qiang; Gan, Xuetao; Zhao, Jianlin

All-optically controlled slow and fast lights in graphene-coated tilted fiber Bragg grating

Published in:
Applied Physics Express

DOI:
10.7567/1882-0786/ab281b

Published: 01/01/2019

Document Version
Peer-reviewed accepted author manuscript, also known as Final accepted manuscript or Post-print

Please cite the original version:
Wang, Y., Jiang, B., Das, S., Zhao, Q., Gan, X., & Zhao, J. (2019). All-optically controlled slow and fast lights in graphene-coated tilted fiber Bragg grating. *Applied Physics Express*, *12*(7), Article 072010. https://doi.org/10.7567/1882-0786/ab281b

All-optically controlled slow and fast lights in graphene coated tilted fiber Bragg grating

Yadong Wang[1,2], Biqiang Jiang[1], Sosubhan Das[2], Qiang Zhao[3], Xuetao Gan[1,*], and Jianlin Zhao[1,*]

[1]*MOE Key Laboratory of Material Physics and Chemistry Under Extraordinary Conditions, and Shaanxi Key Laboratory of Optical Information Technology, School of Science, Northwestern Polytechnical University, Xi'an 710072, China*

[2]*Department of Electronics and Nanoengineering, Aalto University, Espoo 02150, Finland*

[3]*China Academy of Space Technology, Qian Xuesen laboratory of Space Technology, Beijing, China*

*E-mail: xuetaogan@nwpu.edu.cn; jlzhao@nwpu.edu.cn

We demonstrate all-optically controlled slow and fast lights in tilted fiber Bragg grating (TFBG) with a graphene film. By employing graphene's efficient photothermal effect, the global resonances in TFBG are shifted with slopes of 1.1 pm/mW and 1.01 pm/mW for cladding and core modes, respectively. It enables changes of group delay and thus supports tunable fast and slow lights from -156 to 20 ps at cladding modes and up to 400 ps at core modes. Our demonstration with all-in-fiber scheme possesses advantages with low-cost manufacture, simple and compact configuration, and multi-wavelength operations.

The technique to accelerate or delay the light signal is one of the fundamental building blocks in signal processors and optical communication networks, which has attracted lots of interests for a long time.[1, 2)] Realizing tunable velocity for optical data signals directly in fibers is certainly a very promising approach for optimizing of data flow in future optical networks.[3)] The fiber based distributed Bragg reflector (DBR) structures, such as fiber Bragg grating (FBG), are featured with spectral resonances, which not only have been widely used as wavelength selection and encoding in all-in-fiber optical communications,[4, 5)] but also enable superior platforms for tuning the slow light or fast light.[6, 7)] In fact, many methods have been employed as external elements to control group delay with DBR based fibers, such as mechanical strain,[8, 9)] and electric heater.[10-12)] Compared with above techniques, all-optical strategy is more desirable with advantages of noncontact, simple implementation and high stability. By introducing gap-soliton in FBG, the all-optical control of slow lights have been successfully achieved, though suffering high pump power around ~2 kW and narrow bandwidth (~200 MHz).[13)] Doping fibers with active media such as color centers, transition metal ions, or rare earth elements, could support efficient control of FBG resonance with low power consumption, relying on ground state depletion, or photothermal effect. Especially, the chirped FBG and tilted FBG (TFBG) provide superior alternatives with wider operation bandwidth.[14, 15)] For example, low-power pump tuned fast (-38 ps) and slow (18 ps) lights with 22-GHz bandwidth have been successfully realized in TFBG through the erbium's photothermal effect.[15)]

Recently, graphene's photothermal effect has attracted lots of interests.[16-18)] Owing to zero bandgap and linear dispersion of band structure, graphene has wide-band absorption and efficient electron-phonon interaction, thus enabling high photothermal conversion efficiency.[19)] Combining with its natural flexibility and compatible integration with fibers, graphene has been employed as an excellent active material by coating microfiber and micro-FBG for functional devices, such as phase shifter,[17)] optical switching.[20-23)]

In this paper, we employ a few-layered graphene as an active media to control the time delay in a TFBG by all-optical method. The TFBG is used to couple the light into fiber cladding where the guided light will be absorbed by graphene and converted into the Joule heat. The effective refractive index of TFBG is changed due to the thermal-optic effect of silica. Therefore the group delay of the graphene coated TFBG (GTFBG) can be optically controlled, which has great potential in the field of advanced signal processing.

As shown in Fig. 1(a), we wrapped the five-layered graphene onto the grating region of a TFBG. The layer number of graphene was distinguished by transmission electron

microscope and Raman spectrum.[24] The graphene was grown on copper foils via chemical vapor deposition method. After removing copper foils with $Fe(NO_3)_3$ solution, the graphene film can be directly wrapped on a 6-degree TFBG through wetting transfer method.[25] Figure 1(b) shows the image of GTFBG by the scanning electron microscopy, confirming tight joint of graphene and TFBG.

The TFBG belongs to the short-period gratings family with the 6° slanted grating planes. Figure 1(c) shows the typical transmission spectrum of the 6° TFBG with a Bragg resonance, and a group of resonances at shorter wavelengths, namely, the guided cladding modes. These cladding modes could cover very broad bandwidth including the high-order diffractions and sidelobes.[4, 26] Once coated with graphene, the boundary condition of the TFBG is changed due to the high refractive index of the graphene. As shown in Fig. 1(d), the envelopes of the cladding modes appear a certain decrease with graphene coating, indicating a strong coupling between graphene and TFBG. While the core mode of TFBG keeps unchanged, indicating there is no interaction between graphene and core mode. For comparison, the dip envelopes of the cladding modes with and without graphene are plotted in the lower part of Fig. 1(e).[25] The coupling loss is calculated by the difference of two dip envelopes, as shown in the upper part of Fig. 1(e). Since the light absorption of graphene is almost flat in broad bandwidth,[17] this Gaussian-like envelope of loss is mainly contributed by phase-matching condition and light coupling density between graphene and TFBG. Even stronger coupling can be achieved by thicker graphene, though at the expense of insertion loss.

To demonstrate all-optically controlled TFBG, we coupled an extra pump light of 980-nm laser into the GTFBG, accompanying a tunable laser (linewidth: 400 kHz) as a signal light.[20, 21] Note that the operation wavelength of pump light could range with a broad bandwidth. By scanning the signal light (power: 2.5 mW) from wavelength of 1532 nm to 1557 nm, we measured the transmittances of GTFBG with the pump light (power: 240 mW) turned off and on, as shown in Fig. 2(a). The curve presents red-shifts of the global resonances including the cladding (~0.27 nm) and core mode (~0.24 nm) in GTFBG. While the resonance depths of whole spectrum keep constant, which indicates the unchanged absorbance of graphene. For the comparison, we did the reference experiments with bare TFBG. As shown in Fig. 2(b), the global spectrum rarely shifts (~0.02 nm) with pump power of 500 mW. Apparently, the large red shifts in GTFBG (Fig. 2(a)) are contributed by graphene. With the pump excitation, the high-order scattering of grating in TFBG can reflect 980-nm light, which would be coupled into the cladding and then be absorbed by graphene. The graphene induced absorption at 980 nm is measured as ~0.7 dB. Finally, the absorbed

energy can be directly transferred into the Joule heating.[17] Since the thermal-optic effect of silica, fiber's refractive index increases with the temperature (~10^{-5} /K), shifting the resonances of TFBG to longer wavelengths. While the little shift in bare TFBG (Fig. 2(b)) may be contributed by impurity absorption,[27, 28] it exhibits negligible impact with respect to the graphene's photothermal effect.

Specifically, Figs. 2(c)-(e) display the shifted resonances at wavelengths of 1536 nm, 1548 nm, and 1554 nm with continuously increased pump powers. All of the red-shifts behave good linear relations with the pump powers, which are consistent with the thermo-optic nonlinearity.[17] While the fitted slopes decrease from 1.1 pm/mW, 1.06 pm/mW, to 1.01 pm/mW, corresponding to the wavelengths of high-order cladding mode (1536 nm), low-order cladding mode (1548 nm), and core mode (1554 nm) in TFBG, respectively. It is known that the light field distributions in TFBG are decreased from cladding mode to core mode.[29] For lower-order mode, less amounts of evanescent fields opearate outside of the cladding boundary. The most confined mode is core mode, which does not interference with external environment. Thus the measured slopes decrease with the confiner light field. This can be explained by the heat distribution in cross profile of the optical fiber.[29] The Joule heat generated in graphene dissipates from the surface to the fiber core, where the distribution of effective heat intensity would decrease, resulting in decrease of slope at confiner mode.

After understanding the mechanism of optically shifted resonance of GTFBG, we start to consider the group delay of the resonances. In TFBG, each resonance in the cladding and core modes represents a strong variation of group delay, which is similar to dispersion of an absorption or gain medium.[11, 30] The relevant change of the effective group index enbles the slow or fast light. Particularly, fast light happens in the central dip of the resonances, while the pulse can be slowed down at the edges of the resonance peaks.[11, 15] Thus tuning the time delay of signal at certain wavelength can be achieved by shifting the resonance across this wavelength.

To observe tunable slow and fast lights, we built an experimental setup as shown in Fig. 3(a). The light from the tunable laser (TL) is optimized by the polarization controller (PC) to suitable polarization of electro-optic modulator (EOM). The data timing generator (DTG) working on the EOM is employed to generate the non-return-to-zero (NRZ) signal. Then the modulated light is split into 5/95 by an optical fiber coupler (OC), where 95% of the light works as a signal light, and the rest is directly sent to photodetector (PD1) of the oscilloscope (OSC) as a reference. The pump and modulated signal are combined by a 980/1550 nm wavelength division multiplexing (WDM) before the GTFBG. The output signal after the

second WDM is guided to the second photodetector (PD2) of the OSC. The insertion loss of signal is ~5.8 dB, including the EOM, OC, WDMs, and that of 980-nm pump is ~0.3 dB with WDM.

In the experiment, we set the data rate of DTG as 1.26 GS/s (~0.789 ns). Figure 3(b) shows the GTFBG transmission spectrum at resonance around wavelength of 1548.82 nm (insertion loss: ~19.5 dB). As predicted, there would be highest time advancement at the dip of resonance (i.e. around 1548.82 nm) and time delay around the peak (i.e. around 1548.67 nm) in the marked region. Thus the wavelength of 1548.82 nm is chosen for the largest tuning range. In the experiment, the signal power is kept low as 1 mW and the time delay at non-resonance wavelength is recorded as zero time.[15] When gradually increasing the pump power, the time delay of output pulse behaves continuously controllable, as displayed in Fig. 3(c). The curve shows the time advance of -156 ps when pump power is 0 mW, and it delays up to 19 ps when the pump is 180 mW. Here the half values (0.5) of rise edge in the time traces are collected. The tuning bandwidth is around 47 GHz (~0.38 nm red shift at 1548.8 nm) when the pump power is increased to 360 mW. So the time-bandwidth product is around 8.5.[15] Figure 3(d) shows the time traces of the pulses at 1548.82 nm with and without pump power of 180 mW, where the pump light induced pulse delay can be clearly observed. While the time trace of reference at zero delay is also plotted as a reference with red dotted curve. Some distortions exist at the drop edges of pulses, which are mainly contributed by the magnitude and group delay ripples from TFBG.[14] However, by comparison, the pump excitation does not introduce more distortions.

It is also beneficial to actively control the time delay of the core mode in GTFBG without any insertion loss. Figure 4 shows the responses of time delay at the edges of core mode with continuously pump powers. The delay time at the non-resonance position is chosen as the time of zero. The time delay evolution at wavelength of 1554.81 nm with respect to the pump power in the range 0-120 mW is plotted in Fig. 4(a), while the insertion loss here is around 11.6 dB. The inset is the spectrum of left-side core mode. With the increased pump power, the spectrum in the marked region would shift to the position of yellow dotted line, and thus the dispersion at wavelength of 1554.81 nm can be changed. The corresponding time delay decreases from 200 ps to 20 ps with pump power ranging from 0 to 42 mW. Meanwhile, there is a peak when the pump power is around 28 mW, which would be contributed by the chirp in the left-side core mode of TFBG (as shown in inset spectrum).[31] At the right-side core mode, the delay time at wavelength of 1556 nm (insertion loss: 1.7 dB) starts with several oscillations, then increases to a largest peak around 400 ps when the pump power

reaches to 188 mW. The three oscillating ripples when the pump powers range from 40 mW to 150 mW, are caused by chirped resonances corresponding to the peaks of the spectrum shown in inset of Fig. 4(b). All of the time traces are coincident to the feature of resonance edge dispersion in FBG.[31, 32] Meanwhile, different behaviors in two edge-sides of core mode are mainly due to the asymmetric dispersions of core-mode, which can be identified from the different shapes of spectrum in GTFBG.

In conclusion, we have introduced graphene's photothermal effect to actively control slow and fast light in TFBG. With pump, it enables red-shifts of the global spectrum in GTFBG, where the shifted cladding (core) mode has a slope of 1.1 (1.01) pm/mW, which describes heat dissipation phenomenon from surface to the core of GTFBG. The tunable group delays of pulses have been successfully achieved with tunable delay from fast light of -156 ps to slow light of 20 ps at the cladding mode, as well as tunable slow light up to 400 ps at the core mode. This simple, feasible, broad-bandwidth, cost-effective, actively-tunable slow and fast light approach promises potential applications of developing tunable optical memories, and optical data synchronizations. Furthermore, our design by employing graphene as an active media could be suitable to other platforms such as on-chip devices for tunable slow and fast light.[33, 34]

Acknowledgments

Key Research and Development Program (Grant No. 2017YFA0303800), NSFC (Grant Nos. 61775183, 11634010, 61505249, 61775182), Key Research and Development Program in Shaanxi Province of China (Grant Nos. 2017KJXX-12, 2018JM1058) and the Fundamental Research Funds for the Central Universities (Grant No. 3102018jcc034).

References

1) R. W. Boyd, and D. J. Gauthier, Science **326**, 1074-1077 (2009).

2) L. Ren, Y. Xu, C. Ma, Y. Wang, X. Kong, J. Liang, H. Ju, K. Ren, and X. Lin, Journal of Physics: Conference Series **680**, 012032 (2016).

3) L. Thévenaz, Nat. Photon. **2**, 474-481 (2008).

4) K. O. Hill, and G. Meltz, J. Lightwave Technol. **15**, 1263-1276 (1997).

5) D. Mao, Z. He, H. Lu, M. Li, W. Zhang, X. Cui, B. Jiang, and J. Zhao, Opt. Lett. **43**, 1590-1593 (2018).

6) G. Skolianos, A. Arora, M. Bernier, and M. Digonnet, J. Phys. D **49**, 463001 (2016).

7) X. D. Gu, A. Suzuki, A. Matsutani, and F. Koyama, Appl. Phys. Express **7**, 114101

(2014).
8) Y. Q. Liu, J. L. Yang, and J. P. Yao, IEEE Photon. Tech. Lett. **14**, 1172-1174 (2002).
9) C. Caucheteur, A. Mussot, S. Bette, A. Kudlinski, M. Douay, E. Louvergneaux, P. Megret, M. Taki, and M. Gonzalez-Herraez, Opt. Express **18**, 3093-3100 (2010).
10) M. Pisco, S. Campopiano, A. Cutolo, and A. Cusano, IEEE Photon. Tech. Lett. **18**, 2551-2553 (2006).
11) M. Pisco, A. Ricciardi, S. Campopiano, C. Caucheteur, P. Megret, A. Cutolo, and A. Cusano, Opt. Express **17**, 23502-23510 (2009).
12) D. Kinet, C. Caucheteur, M. Wuilpart, P. Megret, and M. Gonzalez-Herraez, IEEE Photon. Tech. Lett. **24**, 557-559 (2012).
13) J. T. Mok, C. M. de Sterke, I. C. M. Littler, and B. J. Eggleton, Nat. Phys. **2**, 775-780 (2006).
14) H. Shahoei, M. Li, and J. P. Yao, J. Lightwave Technol. **29**, 1465-1472 (2011).
15) H. Shahoei, and J. P. Yao, IEEE Photon. Tech. Lett. **24**, 818-820 (2012).
16) S. Ghosh, D. L. Nika, E. P. Pokatilov, and A. A. Balandin, New J. Phys. **11**, 095012 (2009).
17) X. Gan, C. Zhao, Y. Wang, D. Mao, L. Fang, L. Han, and J. Zhao, Optica **2**, 468 (2015).
18) C. Z. Yuan, W. Zhang, and Y. D. Huang, Appl. Phys. Express **11**, 072503 (2018).
19) C. H. Lui, K. F. Mak, J. Shan, and T. F. Heinz, Phys. Rev. Lett. **105**, 127404 (2010).
20) Y. Wang, X. Gan, C. Zhao, L. Fang, D. Mao, Y. Xu, F. Zhang, T. Xi, L. Ren, and J. Zhao, Appl. Phys. Lett. **108**, 171905 (2016).
21) X. Gan, Y. Wang, F. Zhang, C. Zhao, B. Jiang, L. Fang, D. Li, H. Wu, Z. Ren, and J. Zhao, Opt. Lett. **41**, 603-606 (2016).
22) Y. Meng, L. Deng, Z. Liu, H. Xiao, X. Guo, M. Liao, A. Guo, T. Ying, and Y. Tian, Opt. Express **25**, 18451-18461 (2017).
23) Z. Liu, Y. Meng, H. Xiao, L. Deng, X. Guo, G. Liu, Y. Tian, and J. Yang, Opt. Commun. **428**, 77-83 (2018).
24) M. Qi, Y. Zhou, F. Hu, X. Xu, W. Li, A. Li, J. Bai, and Z. Ren, J. Phys. Chem. C **118**, 15054-15060 (2014).
25) B. Jiang, X. Lu, X. Gan, M. Qi, Y. Wang, L. Han, D. Mao, W. Zhang, Z. Ren, and J. Zhao, Opt. Lett. **40**, 3994 (2015).
26) J. Albert, L. Shao, and C. Caucheteur, Laser Photonics Rev. **7**, 83-108 (2013).
27) M. Delgado-Pinar, I. L. Villegas, A. Diez, J. L. Cruz, and M. V. Andres, Opt. Lett. **39**,

6277-6280 (2014).
28) X. Rosello-Mecho, M. Delgado-Pinar, J. L. Cruz, A. Diez, and M. V. Andres, Opt. Lett. **43**, 2897-2900 (2018).
29) T. Guo, F. Liu, B.-O. Guan, and J. Albert, Opt. Laser Technol. **78**, 19-33 (2016).
30) Y. Okawachi, M. S. Bigelow, J. E. Sharping, Z. Zhu, A. Schweinsberg, D. J. Gauthier, R. W. Boyd, and A. L. Gaeta, Phys. Rev. Lett. **94**, 153902 (2005).
31) K. Qian, L. Zhan, H. Li, X. Hu, J. Peng, L. Zhang, and Y. Xia, Opt. Express **17**, 22217-22222 (2009).
32) D. Janner, G. Galzerano, G. D. Valle, P. Laporta, S. Longhi, and M. Belmonte, Phys. Rev. E Stat. Nonlin. Soft. Matter. Phys. **72**, 056605 (2005).
33) F. Y. Sun, L. P. Xia, C. B. Nie, C. Y. Qiu, L. L. Tang, J. Shen, T. Sun, L. Y. Yu, P. Wu, S. Y. Yin, S. H. Yan, and C. L. Du, Appl. Phys. Express **12**, 042009 (2019).
34) C. T. Phare, Y. H. D. Lee, J. Cardenas, and M. Lipson, Nat. Photon. **9**, 511 (2015).

Figure Captions

Fig. 1. (a) Schematic diagram of the graphene coated TFBG (GTFBG). (b) Image of GTFBG by scanning electron microscopy. (c) Transmission spectrum of TFBG. (d) Transmission spectrum of GTFBG. (e) Comparison dip envelopes of transmitted intensity in TFBG with and without graphene. The upper blue curve is the difference of two dip envelopes indicating the graphene's insertion loss.

Fig. 2. Comparison of transmission spectra of GTFBG (a) and TFBG (b) without (black curve) and with (red curve) pump excitation. Insert: one scaled-up resonance of GTFBG and TFBG, respectively. (c)-(e) Pump power dependence of the red-shifted transmission resonances at 1536 nm, 1548 nm, 1554 nm.

Fig. 3. (a) Experimental setup for optically controlling slow and fast light of GTFBG. (b) Transmitted resonance spectrum around wavelength of 1548.8 nm. The dotted line is the wavelength of signal and the marked spectrum would shift to the set wavelength with increased pump powers. (c) Delay times of signal at wavelength of 1548.82 nm with gradually increased pump powers. (d) Normalized time traces at wavelength of 1548.82 nm when pump power is 0 mW (black curve) and 190 mW (red curve) compared with the 0 ps time trace (red dotted curve).

Fig. 4. Actively controlled slow lights at core mode of GTFBG. Delay times of signal at left-side of core mode at wavelength of 1554.81 nm (a) and right-side of core mode at wavelength of 1556 nm (b) when pump powers are gradually increased. The inset shows the spectra at sides of the core mode (left side in (a), right side in (b)) in GTFBG.

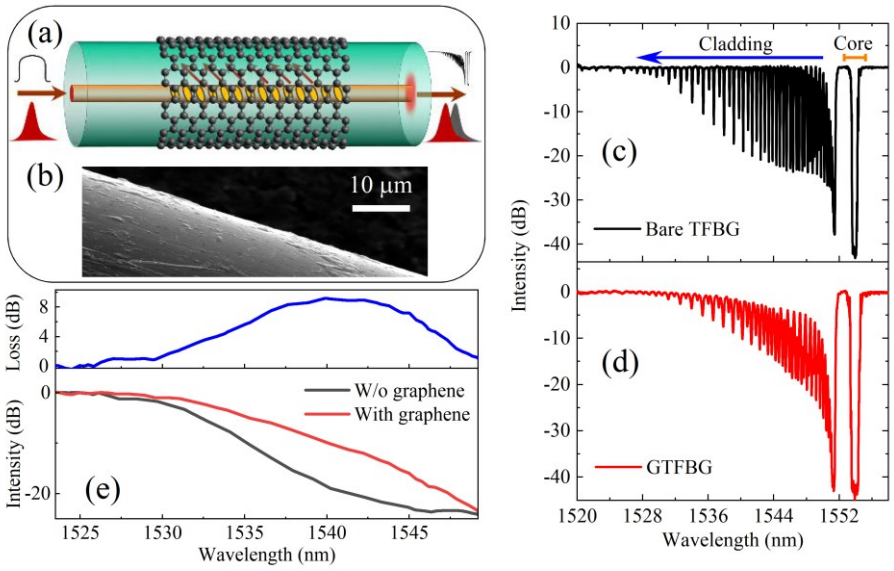
(a)
(b)
10 μm
Loss (dB)
8
4
0
Intensity (dB)
0
-20
W/o graphene
With graphene
(e)
1525
1530
1535
1540
1545
Wavelength (nm)
Cladding
Core
10
0
-10
-20
-30
-40
(c)
Bare TFBG
Intensity (dB)
(d)
GTFBG
1520
1528
1536
1544
1552
Wavelength (nm)

Fig.1.

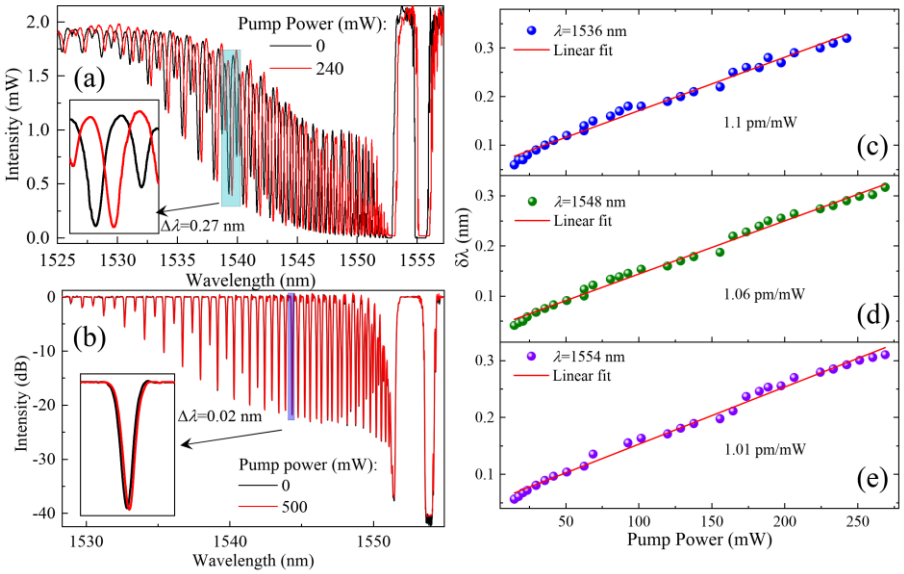
Pump Power (mW):
0
240
(a)
Δλ=0.27 nm
Intensity (mW)
Wavelength (nm)
(b)
Δλ=0.02 nm
Pump power (mW):
0
500
Intensity (dB)
Wavelength (nm)
λ=1536 nm
Linear fit
1.1 pm/mW
(c)
λ=1548 nm
Linear fit
1.06 pm/mW
(d)
λ=1554 nm
Linear fit
1.01 pm/mW
(e)
δλ (nm)
Pump Power (mW)

Fig. 2.

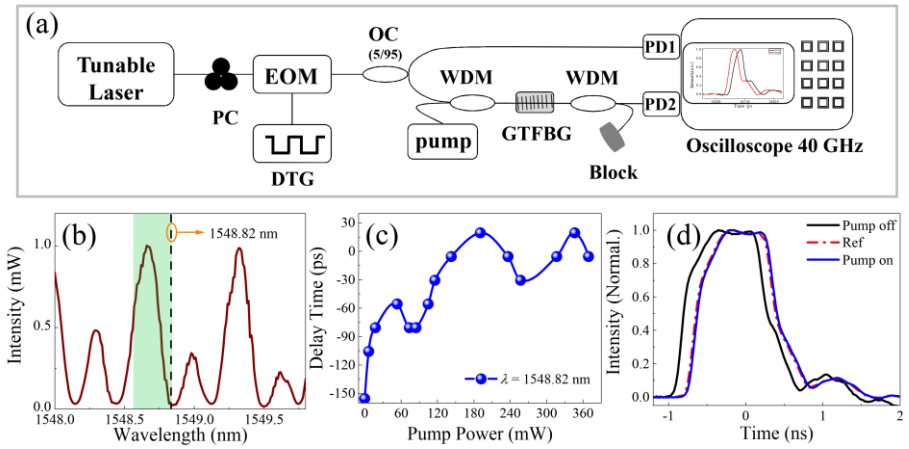
(a)
Tunable Laser
PC
EOM
DTG
OC
(5/95)
WDM
WDM
pump
GTFBG
Block
PD1
PD2
Oscilloscope 40 GHz
(b)
1548.82 nm
Intensity (mW)
Wavelength (nm)
(c)
Delay Time (ps)
λ = 1548.82 nm
Pump Power (mW)
(d)
Pump off
Ref
Pump on
Intensity (Normal.)
Time (ns)

Fig. 3.

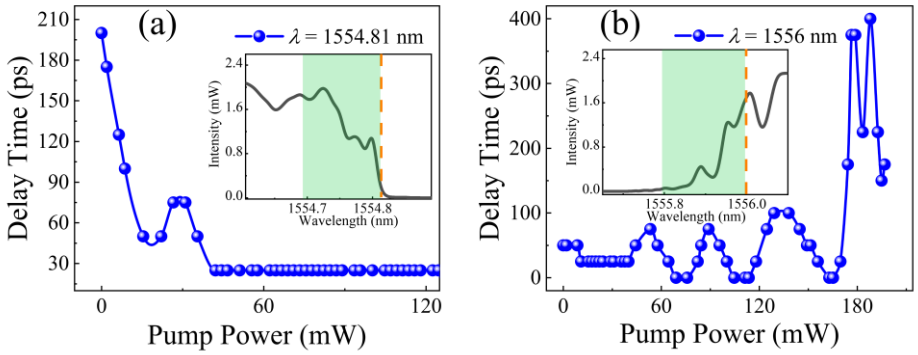
(a)
λ = 1554.81 nm
Delay Time (ps)
Pump Power (mW)
Intensity (mW)
Wavelength (nm)
(b)
λ = 1556 nm
Delay Time (ps)
Pump Power (mW)
Intensity (mW)
Wavelength (nm)

Fig. 4.